General Disclaimer

One or more of the Following Statements may affect this Document

- This document has been reproduced from the best copy furnished by the organizational source. It is being released in the interest of making available as much information as possible.

- This document may contain data, which exceeds the sheet parameters. It was furnished in this condition by the organizational source and is the best copy available.

- This document may contain tone-on-tone or color graphs, charts and/or pictures, which have been reproduced in black and white.

- This document is paginated as submitted by the original source.

- Portions of this document are not fully legible due to the historical nature of some of the material. However, it is the best reproduction available from the original submission.

X-911-75-69
PREPRINT

NASA TM X- 70962

VERTICAL TEMPERATURE AND DENSITY PATTERNS IN THE ARCTIC MESOSPHERE ANALYZED AS GRAVITY WAVES

I. J. EBERSTEIN
J. S. THEON

MARCH 1975

GSFC
GODDARD SPACE FLIGHT CENTER
GREENBELT, MARYLAND

VERTICAL TEMPERATURE AND DENSITY PATTERNS IN THE ARCTIC MESOSPHERE ANALYZED AS GRAVITY WAVES

I. J. Eberstein
Upper Atmosphere Branch
J. S. Theon
Meteorology Branch
Atmospheric & Hydrospheric
Applications Division

ABSTRACT

Three series of rocket soundings were conducted from high latitude sites during winter. In the first series, four pitot pressure soundings were launched during a 13 hour period from Ft. Churchill, Canada (59^{o}N) on January 31, and Feb. 1, 1967. The second series consisted of one pitot sounding and two acoustic grenade soundings carried out during a three hour period on January 13-14, 1970. Temperature and wind profiles and one density profile were observed independently to obtain the thermodynamic structure, the wind structure, and thus their interdependence in the mesosphere. The third series of soundings was conducted from Point Barrow, Alaska (71^{o}N) on December 6, 1971. This series consisted of five soundings of which the first two and the last two were pitot-grenade pairs. Temperature profiles from all soundings in each series were averaged, and a smooth curve (or series of smooth curves) drawn through

the points. A hydrostatic atmosphere based on the average, measured temperature profile was computed, and deviations from the mean atmosphere were analyzed in terms of gravity wave theory. The vertical wavelengths of the deviations were 10-20 km, and the wave amplitudes slowly increased with height. The experimental data were matched by calculated gravity waves having a period of 15-20 minutes and a horizontal wavelength of 60-80 km. Our interpretation is generally consistent with the results of others who have studied gravity-acoustic waves in the atmosphere. The wind measurements are consistent with the thermodynamic measurements. The results also suggest that gravity waves travel from East to West with a horizontal phase velocity of approximately 60 m sec^{-1}.

CONTENTS

ILLUSTRATIONS

TABLES

SYMBOLS

ω = circular frequency of the wave

a = local sound speed

$k_0 = \omega/a$

γ = ratio of specific heats

$\omega_B = g/a \sqrt{\gamma - 1}$ = Brunt - Vaisala frequency

$\omega_A = \gamma g/2a = a/2H$

g = acceleration due to gravity

H = Pressure scale height

$A = \omega_A / \omega$

$B = \omega_B / \omega$

$S = k_x/k_0$

$G = \omega_h / \omega$

$\omega_h = a^2/2k$

k = thermal diffusivity

$\vec{U}$ = wind velocity of background field

$\vec{k}$ = propagation vector

$k^2 = k_x^2 + k_z^2$

P = static pressure

P^0 = stagnation pressure

ρ = density

u = velocity

INTRODUCTION

Waves in a stratified fluid under the influence of gravity appear to have been initially discussed by Burnside (1889) and Love (1891). Both authors treated an incompressible fluid. Görtler (1943) used schlieren photography to show experimentally that disturbances in an incompressible stratified medium under the influence of gravity propagate along characteristic rays. Lamb (1909) treated a compressible, adiabatic, ideal gas whose density is stratified by gravity. Since the early contributions by Burnside, Love, and Lamb, there have been many theoretical papers on various types of gravity waves. Reasonably up-to-date treatments of the subject may be found in Eckart (1960) and Yih (1965). However, gravity wave theory is currently undergoing an active phase of development and contributions are being added to the literature at a rapid rate. A recent addition is the book by Tolstoy (1973).

The present paper treats several series of rocket soundings of atmospheric temperature, density, and wind structure. The experimental results are interpreted in terms of gravity-acoustic wave theory. The experiments are of two types, pitot and grenade. For the pitot experiment, a pitot stagnation probe is mounted on the rocket vehicle. The position and velocity of the vehicle are measured by radar tracking. For an incompressible fluid, we have the simple formula

$$P^0 = P + 1/2\, \rho\, u^2 \qquad (1)$$

where P^0 is stagnation pressure

P is static pressure

ρ is density

u is velocity

Eq. (1) may also be written in the form:

$$\rho = \frac{2(P^0 - P)}{u^2} \qquad (1a)$$

It is obvious from Eq. 1a that density is determined if stagnation pressure, static pressure, and velocity are measured. The addition of compressibility makes the analysis somewhat more involved without affecting the basic principle presented above. The pitot technique is described in detail by Horvath et. al (1962).

For the grenade experiment, a series of grenades are exploded in the atmosphere. The position and time of the explosion is determined and the time, and the direction of arrival of the spherical sound pulse are measured by a ground based microphone array. This information is used to deduce the mean temperature and horizontal wind speed in atmospheric slabs whose thickness varies between 2 km and 4 km depending on the particular grenade payload used. (Nordberg and Smith, 1964)

Essentially, the pitot technique provides a high vertical resolution (0.5 km) direct measurement of atmospheric density, while the grenade technique gives a direct measure of atmospheric temperature and horizontal wind with a 2-4 km vertical resolution. For both techniques, the time to make the

atmospheric traverse is approximately one minute, resulting in a virtually instantaneous picture of the vertical structure.

EXPERIMENTAL PROCEDURE

The experimental data consist of three series of rocket soundings which were conducted from high latitude sites during winter. In the first series, four pitot soundings were launched during a thirteen hour period from Ft. Churchill, Canada (59°N) spanning January 31 and February 1, 1967 (see Table 1). The data have been published by Smith, et al (1969).

The second series consisted of three soundings carried out during a three hour period on January 13-14, 1970 from Churchill (Smith, et. al., 1972) The first sounding was made with the acoustic grenade technique to measure the temperature and wind profiles in the 35-90 km region; the second sounding was a pitot probe launched 88 minutes later to measure the density profile; and the last sounding employed the acoustic grenade technique 104 minutes after the pitot sounding. Thus two temperature and wind profiles and one density profile were obtained independently to permit examination of the thermodynamic structure, the wind structure, and the interdependence of each in the mesosphere.

The third series of soundings was conducted from Point Barrow, Alaska (71°N) on December 6, 1971 (Smith et. al., 1974). This series consisted of five soundings, of which the first two and last two were pitot-grenade pairs. The remaining sounding was performed with a pitot probe. The objective of

launching such pairs was to obtain high vertical resolution thermodynamic structure (pitot) and wind information (grenade) simultaneously. The series commenced at 0300 GMT with a pitot probe, which was followed by a grenade at 0302 GMT. These profiles were flown over essentially the same trajectory only two minutes apart. The remaining soundings, a pitot at 0442 GMT, a pitot at 0752 GMT, and a grenade at 0802 GMT completed the series.

OUTLINE OF GRAVITY WAVE THEORY

Consider a series of layers of fluid, each lighter than the one below, as shown in Figure 1. A surface wave in the lowest layer will transmit a disturbance to the layer above it, which in turn will transmit the disturbance to the layer above it, etc. Now let the density difference between layers and the layer thickness both approach small values ϵ and δ, respectively. In the limit, as ϵ and δ approach zero, we have internal gravity waves. The soundings described above have taken samples vertically through the layers.

The simple theory involves linearizing the atmospheric equations of motion and specifying a sinusoidal solution, i. e.,

$$\phi = \phi_0 \exp\left[i(\omega t - k_x x - k_z z)\right] \qquad (2)$$

Perturbations in pressure, density, temperature, and gravity wave generated wind are related to ϕ by what Hines (1960) has called polarization relations, and a dispersion relation which has the form:

$$n_z^2 = \left\{1 - \left(\frac{\omega_A}{\omega_B}\right)^2\right\} - n_x^2 \left\{1 - \left(\frac{\omega_B}{\omega}\right)^2\right\} \qquad (3)$$

where

$$n_x = \frac{k_x a}{\omega} \qquad n_z = \frac{k_z a}{\omega} \quad . \tag{4}$$

(Pitteway and Hines, 1963)

The following expressions are obtained for phase velocity:

$$V_{px} = \frac{\omega}{k_x} \; ; \; V_{pz} = \frac{\omega}{k_z} = \frac{\omega \lambda_z}{2\pi} = \frac{\lambda_z}{\tau} \tag{5}$$

Also,

$$V_{px} \approx \frac{\lambda_z}{\tau_B}$$

provided that $\tau \gg \tau_B$

Since atmospheric gradients are usually gentle, the ray approximation for vertical wave propagation was used. Volland (1969a) has shown that the ray treatment is a sufficient approximation for gravity waves propagating obliquely upwards, provided the horizontal wave number is in the order of, or greater than ω/a, where a is the sound speed, and ω is the circular frequency of the wave, i.e. $k_x \geq \frac{\omega}{a}$, or $(\omega/a)/k_x \leq 1$. Reference to eq. 5 shows that the last mentioned inequality may be written as $V_{px}/a \leq 1$. Thus the ratio of horizontal phase velocity to sound speed must be less than one.

The above ratio, called VPXA, is plotted in Figure 2. We see that it is relatively insensitive to temperature and wave period, but varies linearly with vertical wave length. For vertical wave lengths less than 15 km, VPXA

is generally less than 0.2. Thus, the condition for use of the ray approximation is well satisfied.

The next problem which comes to mind is how to take account of background wind. The frequency of a moving fluid particle, or the 'intrinsic frequency' may be defined as

$$\Omega = \omega - \vec{k} \cdot \vec{U} \qquad (6)$$

where

$\vec{k}$ is wave number

$\vec{U}$ is wind velocity

ω is wave frequency in a quiescent atmosphere

The above value of intrinsic frequency may be substituted into equations describing gravity wave propagation in a quiescent atmosphere, and a solution obtained. Jones (1969) discusses the conditions under which the above procedure is valid. Basically, the following assumptions must be satisfied:

1. Vertical and horizontal derivatives of vertical winds must be less than $(N^2 - \Omega^2)^{1/2}$, where N is the Brunt-Vaisala frequency.
2. Horizontal derivatives of horizontal winds must be smaller than Ω.
3. Time derivatives of horizontal winds must be much smaller than $(\Omega/\beta) \times (N^2 - \Omega^2)^{1/2}$, where $\beta = N^2/g$.
4. Time derivatives of vertical winds are much smaller than g, the acceleration due to gravity.

Derivatives of winds are not generally known, but we can examine the range which is permitted by the above conditions. Condition "4" places a limit of 9.8 m sec^{-2} to accelerations in vertical motion. Vertical winds generated by gravity waves are generally less than 10 m sec^{-1}. The frequency must be less than the Brunt-Vaisala frequency which is about 0.02^{-1}. The resulting acceleration is 0.2 m sec^{-2}, which is well below gravitational acceleration. Vertical wavelengths for major wind shifts are generally longer than 5 kilometers. Thus, we may approximate the maximum vertical derivative of vertical wind to be of the order of 10 m sec^{-1} per 5 km, or 2 m sec^{-1} km^{-1}. Horizontal derivatives of vertical winds are less, since horizontal wavelengths are longer than vertical ones. For conditions considered in this paper $\Omega < 0.5N$, consequently $\Omega^2 < 0.25N^2$, and to a first approximation, we may simply require that vertical gradients of vertical wind be less than the Brunt-Vaisala frequency, i. e.

$$dV_z/dz < N \tag{7}$$

Cancelling the space dimension, dV_z/dz becomes 0.002 sec^{-1}. N is approximately equal to 0.02 sec^{-1}. Thus condition "1" is amply satisfied.

Conditions "2" and "3" are the problematic ones. Taking $\Omega^2 \ll N^2$, condition "3" simplifies to

$$\frac{dV_H}{dt} \ll g\left(\frac{\Omega}{N}\right) \tag{8}$$

Condition "2" may be written in the form

$$\frac{dV_H}{dx} \ll \Omega \qquad (9)$$

If time and space variations of horizontal winds are due to synoptic phenomena, then the following quantities are characteristic:

$V_H \sim 50$ m sec^{-1}; t $\sim$10,000 sec; dX $\sim$500 km

One can then estimate synoptic time and space derivatives to be 10^{-3} m sec^{-1}, and 10^{-4} sec^{-1}. In the above case, eq. (8) requires (Ω/N) to be greater than 0.001 and eq. (9) requires Ω to be greater than 10^{-4} sec^{-1}.

ANALYSIS OF DATA

Table 1 shows the schedule of the four launches in the first series. The times between launches are, respectively, 6h21m, 2h48m, and 3h32m. Temperature profiles from all soundings in each series were averaged and a smooth curve (or a series of smooth curves) drawn through the points. A hydrostatically determined atmosphere based on the average measured temperature profile was computed. The average temperature profile for the first set of data is given in Figure 3. Average background atmospheres were calculated in a similar manner for the second and third sets of experimental series.

The pitot probe technique provides a measurement of the atmospheric density profile by relating the density to the measured ram pressure using appropriate aerodynamic theory, while the acoustic grenade technique provides a measurement of the atmospheric temperature profile by relating the temperature to the measured speed of sound using gas kinetic theory. The hydrostatic equation and the equation of state are used to obtain the remaining two thermodynamic parameters in each technique. Such an approach assumes that vertical accelerations in the atmospheric motions are negligible relative to the acceleration due to gravity, and is valid for mean atmosphere calculations. Smith, et al (1968) compared the results of grenade soundings and pitot probe soundings at Wallops Island, Va. They found temperature agreement to be better than 3^0K below 60 km and better than 5^0K between 60 and 90 km altitude. Thus hydrostatic equilibrium was valid under the generally undisturbed conditions of Wallops Island, confirming the validity of the hydrostatic approximation for background atmosphere calculations.

For the first test series, the ratio of the density measured by the pitot probe to the hydrostatically computed density (based on the average temperature profile) was plotted as a function of altitude for each probe. The density variations are shown in Figure 4. The second and third soundings show a density minimum at around 110 km. This is most pronounced for the second sounding. The pronounced density drop, associated with a pronounced temperature rise, is quite probably due to an auroral event. The structure below 100 km contains

various features which could conceivably be traced from one sample to the next, but this type of exercise will be left to the interested reader. Rather, the authors matched the experimental curves to results obtained from gravity wave theory. Our program was adapted from one used by Volland (1969 a, b). The periods which result in a reasonable fit are in a range of 15-20 minutes with a horizontal wavelength of 60-80 km. The above values correspond approximately to those found by Gossard (1962) who observed gravity waves in the troposphere. Figure 4 essentially gives only the vertical wavelength, λ_z, thus only allowing one to obtain the product of $\omega\lambda_x$. The reason for choosing the short period, short horizontal wavelength waves, is that these are more strongly damped. Reference to Figure 4 shows that the growth of amplitude with altitude is extremely weak, while theory predicts that an undamped wave will grow exponentially with altitude.

Figure 5 shows the spatial auto correlation function for atmospheric density between 28 and 80 km, and Figure 6 shows the corresponding power spectral density versus wavelength. Analysis techniques employed are discussed in Bendat and Piersol (1966) and Blackman and Tukey (1958). (In this case "power" is defined in terms of wavelength and amplitude). Wavelengths between 2 km and 17 km are represented, with a primary peak around 14 km, and a secondary peak around 9 km. The auto correlation function for the second sounding shows a wavelength of 2 x 7 km, and for the fourth, a wavelength of 2 x 9 km, i. e. 14 km and 18 km, respectively, for the dominant sinusoidal component. Figure 7 shows representative gravity waves propagating in a sinusoidal wind

field, and in a quiescent atmosphere. The regular sinusoidal pattern present in the quiescent atmosphere density deviation with altitude is dramatically altered by the introduction of a regularly varying background wind. Thus in the real atmosphere, it is expected that the regular patterns superimposed on the thermodynamic structure by internal gravity waves will not be obvious. The interactions between propagating waves and varying background conditions are exceedingly complex and cannot be separated readily without a priori knowledge of the conditions.

In the second test series, an attempt to identify propagating internal gravity waves in the mesosphere was made by sounding the region with three instrumented rockets on January 13-14, 1970, from Churchill, Canada (59^{o}N). The three observations, which were conducted at approximately 90 min. intervals, consisted of a pitot probe bracketed by two acoustic grenade soundings. Thus, two temperature and wind profiles and one density profile were obtained independently, permitting an examination of the thermodynamic structure and the wind structure. The first sounding was conducted at 2223 GMT with the acoustic grenade technique to measure the temperature and wind profiles in the 35-90 km region; the second sounding was launched 88 minutes later (2351 GMT) and employed a pitot probe to measure the density profile with 0.5 km vertical resolution; and the last sounding again was made

with the acoustic grenade technique 104 minutes after the pitot sounding (0135 GMT). Thus, two temperature and wind profiles, and one density profile were obtained independently to permit an examination of the thermodynamic structure, the wind structure, and the interdependence of each in the mesosphere. For descriptions of the experiment, see Smith, et. al. (1972).

An average atmosphere was calculated based on the three soundings, and the differences of the pitot data from the mean were computed (these are referred to as perturbations). The observed perturbations are shown as the solid curves in Figure 8 and are seen to give a pattern characteristic of internal gravity waves in a stratified, compressible fluid. Recall that the experimental density is measured directly, while the pressure is a derived quantity. In Figure 8, the period of the calculated gravity wave was 20 minutes, and the horizontal wavelength was 60 km.

Figure 9 shows the comparison between the zonal wind profile measured by the first grenade sounding, and the wind pattern associated with the theoretically calculated gravity wave. (A zonal drift wind varying linearly from 12 m sec^{-1} at 36 km to 44 m sec^{-1} at 96 km has been included). The wind pattern obtained by the second grenade sounding is generally similar. Figure 10 shows the theoretically derived vertical velocity profile, which includes values of approximately 10 m sec^{-1} in the 80 km region. Justus and Edwards (1971) have

reported measured vertical velocities on the order of 20 m sec^{-1} at altitudes between 88-118 km. Although these measurements were made at a different latitude and time of year, they are at least comparable in magnitude. The Justus and Edwards data do confirm the existence of relatively large vertical velocities at high altitudes. The vertical velocity profile given by Figure 10 was included in the data reduction for the two grenade soundings and its effect on the mean profile was found to be small.

The third set of measurements consisted of a series of pitot and grenade soundings from Point Barrow (71°N) launched on December 6, 1971. The first two soundings, a pitot and a grenade, were launched two minutes apart. The temperature perturbation obtained from the pitot profile is shown in Figure 11 together with a theoretical gravity wave which was matched to it for a best fit (by eye). Figure 12 shows a comparison between the theoretical and observed wind patterns. The calculated wind pattern is that associated with the gravity wave whose temperature perturbation is given in Figure 11. A mean drift wind of 40 m sec^{-1} has been included. The measured wind is obtained from the grenade sounding, so it represents a series of values in which the winds were averaged over layers (2-3 km thick) between grenade explosions.

Figures 13 and 14 show the temperature perturbations derived from the observed density structure by the subsequent pitot soundings at 0442 GMT and 0752 GMT, respectively. The gravity wave structure is based upon the original match of Figure 11 and allowed to propagate with time to correspond to

the times of the observational data. The best match was found to have a horizontal wavelength of 70 km and a period of about 18 minutes. It is significant that only the first theoretical curve was fitted to the observed data, and that the remaining matches followed from the computer. Thus our data indicate that not only are the spatial density and wind structure measurements compatible with gravity wave theory, but also with the expected behavior with time.

THE PARABOLIC TRAJECTORY EFFECT

For simplicity of discussion, we have considered a vertical, instantaneous slice through the atmosphere. In fact the actual sample is neither wholly vertical nor quite instantaneous. The latter approximation, however, is very good. The sampling time is one minute, representing only 5% of a wave period. The deviation of the actual trajectory from vertical is a more serious matter. Figure 15 shows a typical pitot probe trajectory. Figure 16 compares a trajectory going into the wave, a trajectory following the wave, and an instantaneous vertical traverse. We see the expected Doppler phenomenon of shortened wavelength going into the wave, and lengthened wavelength when going with the wave.

The wave considered has a horizontal wavelength of 70 km and a period of 18.5 minutes. While the measurements are being made, the horizontal distance traversed by the rocket is 12 km, or 1/6 of a wavelength. Thus, it is

the horizontal motion of the rocket rather than the finite sampling time which results in significant deviation from the original simplifying assumption.

Examination of the experimental curves shows that the wavelength decreases with altitude. Thus the rocket is going into the wave train. Since the launch direction from Pt. Barrow is due east, we may conclude that the wave train is coming from an easterly direction. The same situation prevails at Ft. Churchill. Our results suggest that the waves in these instances travelled from East to West. The horizontal phase velocity is approximately 60 m sec^{-1}.

CONCLUSIONS

Three series of soundings were carried out at high latitude sites during winter. The first series gave four essentially instantaneous vertical density traverses during a 13 hour period at Ft. Churchill. The density variations from the mean stratospheric conditions were matched by gravity waves having vertical wavelengths of 14-17 km. A reasonable fit to the data was obtained with a plane gravity wave characterized by a horizontal wavelength of 70 km and a period of 18 minutes. The wave amplitude increased with altitude, but at a rate much slower than the exponential growth predicted for undamped waves. Thus one must conclude that the waves were heavily damped as they propagated upward through the atmosphere.

Comparing our observations with the damping predictions of Pitteway and Hines (1963), it is found that for the constant viscosity case, (i. e. increasing

kinematic viscosity) waves having the input parameters considered. (i. e. 70 km horizontal wavelength, and 10-20 km vertical wavelength) would tend to reach a peak amplitude at about 120 km altitude. The Pitteway-Hines predictions are consistent with our observations, and their amplitude balance damping case appears to be close to what we observed. The observations indicate a modest growth of amplitude with altitude, much closer to the no-growth approximation than to the exponential growth limit.

Consider now the 70 km horizontal wavelength and the 18 minute period. Gossard (1962) observed gravity waves in the troposphere. He found the period to vary between 15 minutes and 120 minutes. The horizontal wavelength for waves of 15 minute period was 19 km, and for two hour period, it was 150 km. The difference between our observations and those of Gossard may be explained by assuming that tropospheric waves with short vertical wavelengths are damped out. In fact Gossard (1962) found that the maximum leakage into the upper atmosphere occurs at periods of 10 to 20 minutes, starting with a white energy spectrum in the troposphere. Our value of 18 minutes is thus consistent with Gossard's prediction. Gossard found a horizontal phase speed of approximately 21 m sec^{-1}. For an 18 minute period and 200°K, the following table relates our estimated horizontal phase velocity to vertical wavelength. 200 degrees was chosen because it is approximately the temperature at the bottom of our test region.

200^{o}K; 18 minute period

λ_z(km)	λ_x(km)	V_{px}(m/sec)	V_{pz}(m/sec)
5	18.2	16.9	4.6
10	36.4	33.7	9.3
15	54.4	50.4	13.9
20	72.3	67.0	18.5
25	90.0	83.3	23.1

From noctilucent cloud studies, Witt (1962) observed characteristic wavelengths of 30-40 km, and of 75 km, the latter being very nearly the 70 km deduced in the present study. Witt (1962) also estimated the wave velocity with respect to a frame of reference moving with the cloud system, obtaining a range of 70 to 135 m sec^{-1}. The agreement with the values given in our table above is reasonable. Noctilucent clouds are formed in the 80 to 85 km region of the atmosphere.

Our results are also generally consistent with the discussion of internal atmospheric gravity waves at ionospheric heights presented by Hines (1960). Thus the 12 km vertical wavelength which Hines deduced from the meteor wind data of Greenhow and Neufeld (1955, 1959) is in reasonable agreement with our observations. Hines considered 125 m sec^{-1} to be a typical horizontal phase speed and quoted the following experimental results. Munro (1958) found phase speeds to generally be in the range of 52-175 m sec^{-1}, in agreement with both

our deductions and Witt's (1962) noctilucent cloud observations. Heisler (1958) found phase speeds to range between 97-207 m sec^{-1}. The phase speed agreement is remarkable considering that ionospheric heights range up to more than 100 km above the top of our observation regime. Our period is more than ten times shorter than the 200 minutes deduced by Hines (1960) from correlation studies of meteor wind trails. However, a careful reading of Hines' paper suggests that the 200 minutes is an upper limit to the period, rather than a most characteristic value.

The second series of soundings is also compatible with a gravity wave interpretation. Vertical wavelengths were consistent with the values obtained in the first series. There was also reasonable agreement between measured and predicted horizontal velocities.

The results of the third series confirmed the conclusions about vertical wavelength and amplitude of the first two series and the agreement of measured wind with gravity wave predictions. It was also possible to trace one gravity wave pattern through three consecutive samples, indicating that our period is correct. There is, of course, the possibility of aliasing. However, the slow wave growth with altitude points toward the short wavelength, short period solution, as do Witt's observations at noctilucent cloud altitudes.

BIBLIOGRAPHY

Bendat, J. S. and Piersol, A. G. (1966) "Measurement and Analysis of Random Data." Wiley, New York

Blackman, R. B. and Tukey, J. W. (1958) "The Measurement of Power Spectra." Dover

Burnside, W. (1889) On the Small Wave Motion of a Heterogeneous Fluid Under Gravity, Proc. London Math Soc. pp. 392-397

Eckart, Carl (1960) "Hydrodynamics of Oceans and Atmospheres." New York, Pergamon

Gossard, E. E. (1962) Vertical Flux of Energy into the Lower Ionosphere from Internal Gravity Waves Generated in the Troposphere. J. Geophysical Research, Vol. 67, pp. 745-757

Görtler, H. (1943) Über eine Schwingungserscheinung in Flüssigkeiten mit stabiler Dichteschichtung. Zeitschrift für Angewandte Mathematik end Mechanik. Band 23, Heft 2, pp. 65-71.

Greenhow, J. S. and Neufeld, E. L. (1955) Phil. Mag, 46, 549

Greenhow, J. S. and Neufeld, E. L. (1959) J. Geophys. Res. 64, 2129

Heisler, L. H. (1958) Australian Journal of Physics Vol. 9, p. 324

Hines, C. O. (1960) Internal Atmospheric Gravity Waves at Ionospheric Heights. Canadian Jour. Physics, Vol. 38, pp. 1441-1481

Horvath, J. J., Simmons, R. W., Brace, L. H. (1962) Theory and Implementation of the Pitot-Static Technique for Upper Atmospheric Measurements. Space Physics Research Lab. Scientific Report NS-1 University of Michigan

Jones, W. L. (1969) Ray Tracing for Internal Gravity Waves. J. Geophysical Research, Vol. 74, pp. 2028-2033

Justus, C. G. and Edwards, F. D. (1971) Winds Observed From July 1968 Through November 1970 in the 83 to 216 km Altitude Region. Final Report, AFCRL Contract F 19628-68-C-0081

Lamb, H. (1909) On the Theory of Waves Propagated Vertically in the Atmosphere. Proc. London Mathematical Society, pp. 122-141

Love, E. H. (1891) Wave Motion in a Heterogeneous Heavy Liquid. Proc. London Mathematical Society, pp. 307-316

Munro, G. H. (1958) Australian Journal of Physics, Vol. 9, p. 324

Nordberg, W., and Smith, W. (1964) The Rocket Grenade Experiment. NASA Technical Note D-2107

Pitteway, M. L. V., and Hines, C. O. (1963) The Viscous Damping of Atmospheric Gravity Waves. Canadian Jour. Physics, Vol. 41, pp. 1935-1948

Smith, W. S., Katchen, L. B., and Theon, J. S. (1968) Grenade Experiments in a Program of Synoptic Meteorological Measurements. Meteorological Monographs, Vol. 8, No. 31, pp. 170-175

Smith, W. S., Theon, J. S., Swartz, P. C., Casey, J. F., Horvath, J. J. (1969) Temperature, Pressure, Density and Wind Measurements in the Stratosphere and Mesosphere, 1967. NASA TR-R-316

Smith, W. S., Theon, J. S., Wright, D. U., Casey, J. F., Horvath, J. J. (1972) Measurements of the Structure and Circulation of the Stratosphere and Mesosphere, 1970. NASA TR-R-391

Smith, W. S., Theon, J. S., Wright, D. U., Ramsdale, D. J., Horvath, J. J. (1974) Measurements of the Structure and Circulation of the Stratosphere and Mesosphere, 1971-72. NASA TR-R-416

Tolstoy, I. (1973) "Wave Propagation," McGraw Hill

Volland, H. (1969, a) Full Wave Calculation of Gravity Wave Propagation Through the Thermosphere. J. Geophysical Research, Vol. 74, pp. 1786-1795.

Volland, H. (1969, b) The Upper Atmosphere as a Multiple Refractive Medium for Neutral Air Motions. J. Atmospheric Terrestrial Physics Vol. 31, pp. 491-514.

Witt, Georg. (1962) Height, Structure and Displacement of Noctilucent Clouds. TELLUS, Vol. 14, pp. 1-18.

Yih Chia-Shun (1965) "Dynamics of Non-Homogeneous Fluids," New York, MacMillan

Table I

Launch Sequence of First Series

Fort Churchill, (59°N); 1967

GMT	Date	Time After First Shot	Type
2317	Jan 31	0h00m	Pitot
0538	Feb 1	6h21m	Pitot
0826	Feb 1	9h09m	Pitot
1158	Feb 1	12h41m	Pitot

Table II

Launch Sequence of Second Series

Fort Churchill (59°N); 1970

GMT	Date	Time After First Shot	Type
2223	Jan 13	0h00m	Grenade
2351	Jan 13	1h28m	Pitot
0135	Jan 14	3h12m	Grenade

Table III

Launch Sequence of Third Series

Point Barrow (71°N); 1971

GMT	Date	Time After First Shot	Type
0300	Dec 6	0h00m	Pitot
0302	Dec 6	0h02m	Grenade
0442	Dec 6	1h42m	Pitot
0752	Dec 6	4h52m	Pitot
0802	Dec 6	5h02m	Grenade

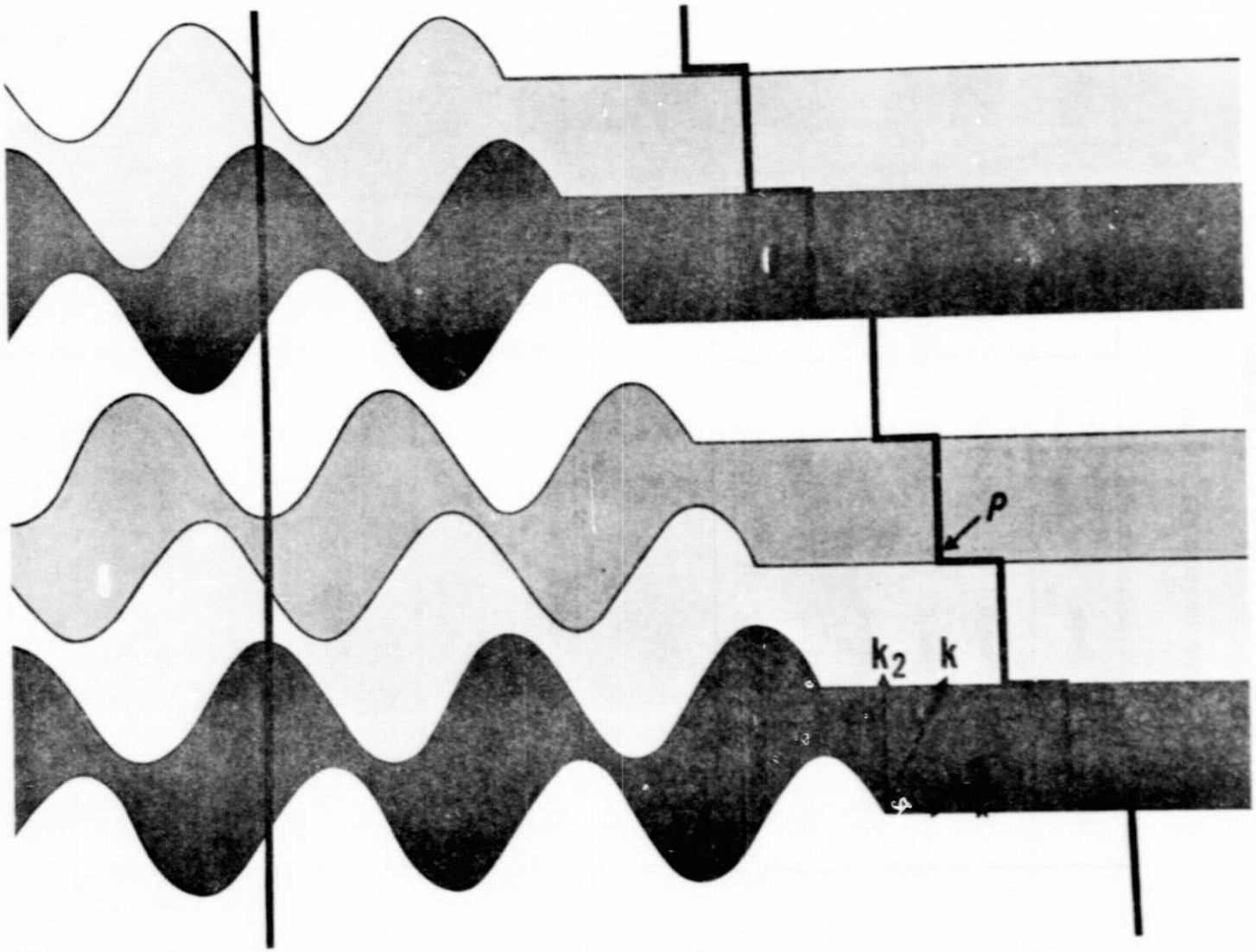

Figure 1. Illustration of Gravity Wave Concept and Nature of Experimental Measurement

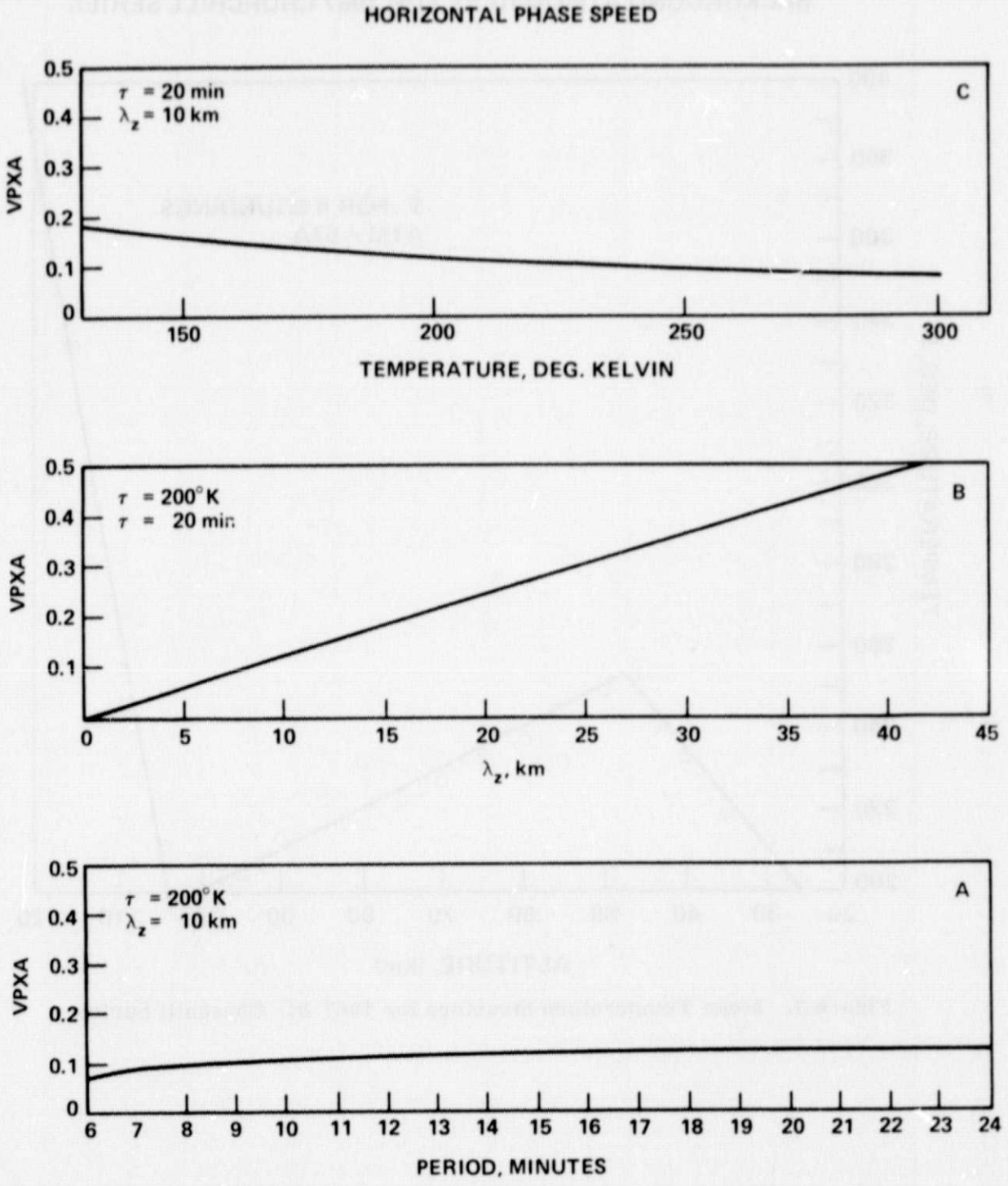

Figure 2. Gravity Wave Phase Speed as Function of Temperature, Vertical Wave Length, and Period

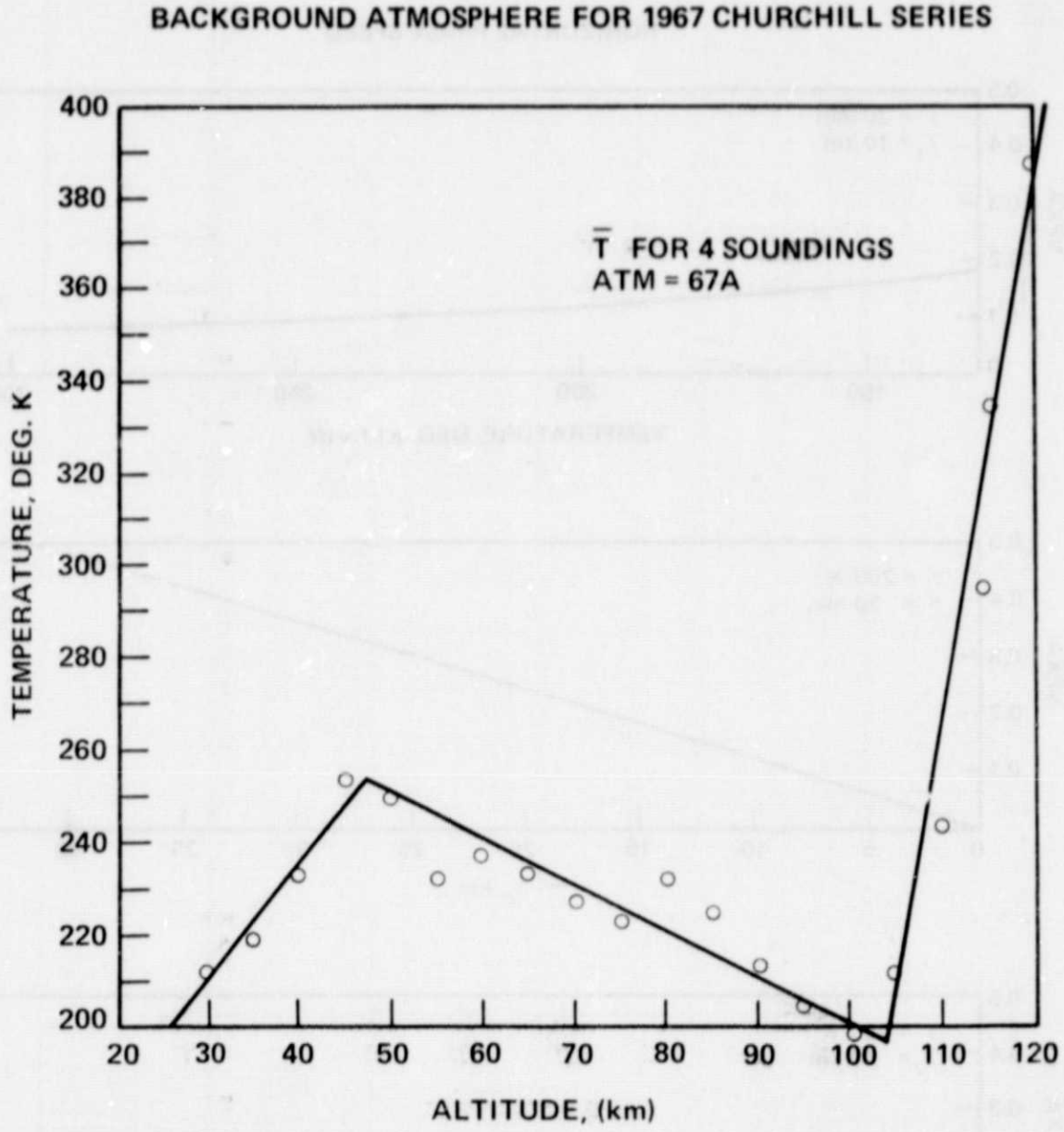

Figure 3. Mean Temperature Structure for 1967 Ft. Churchill Series

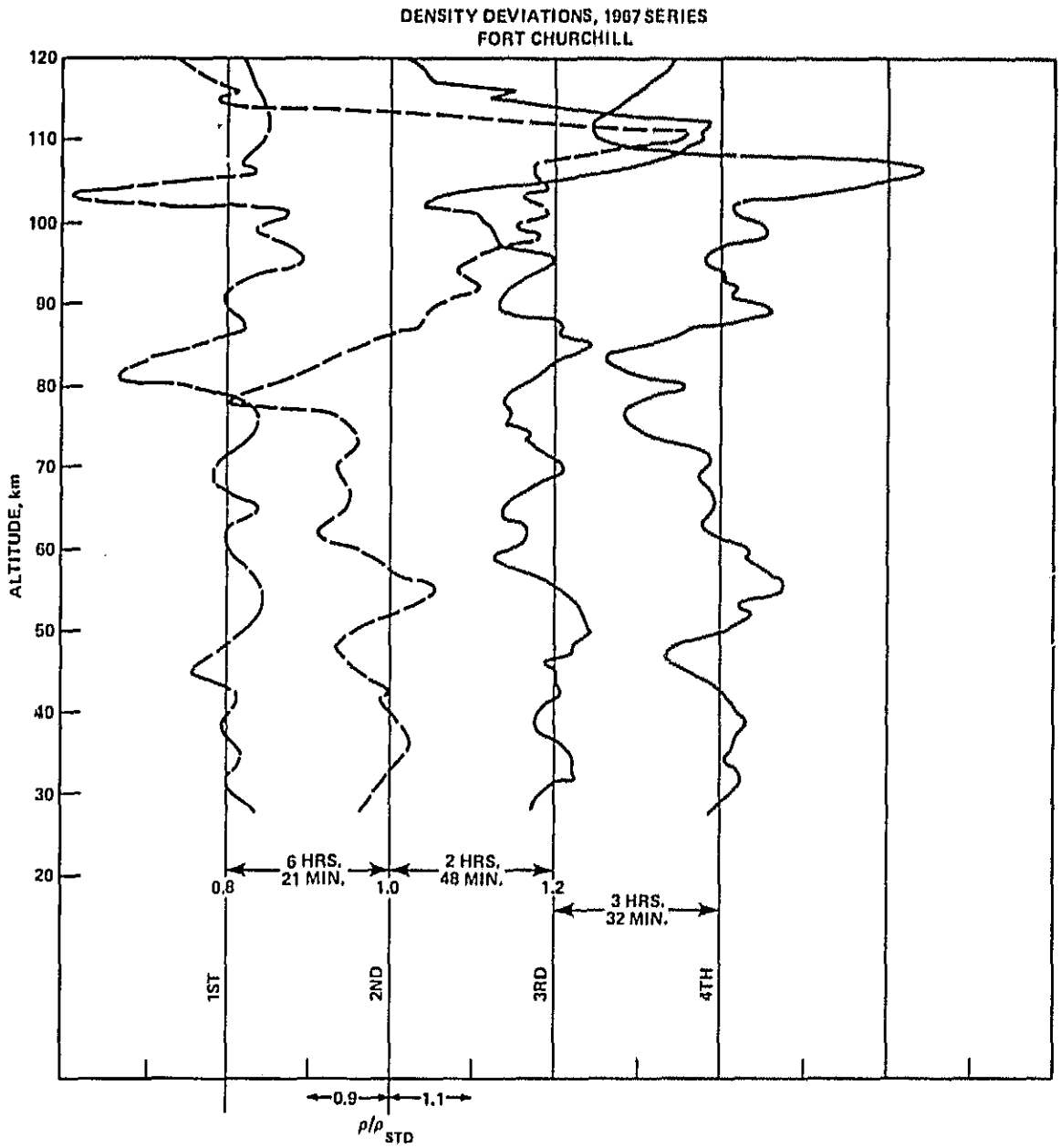

Figure 4. Measured Density Structure for 1967 Ft. Churchill Series

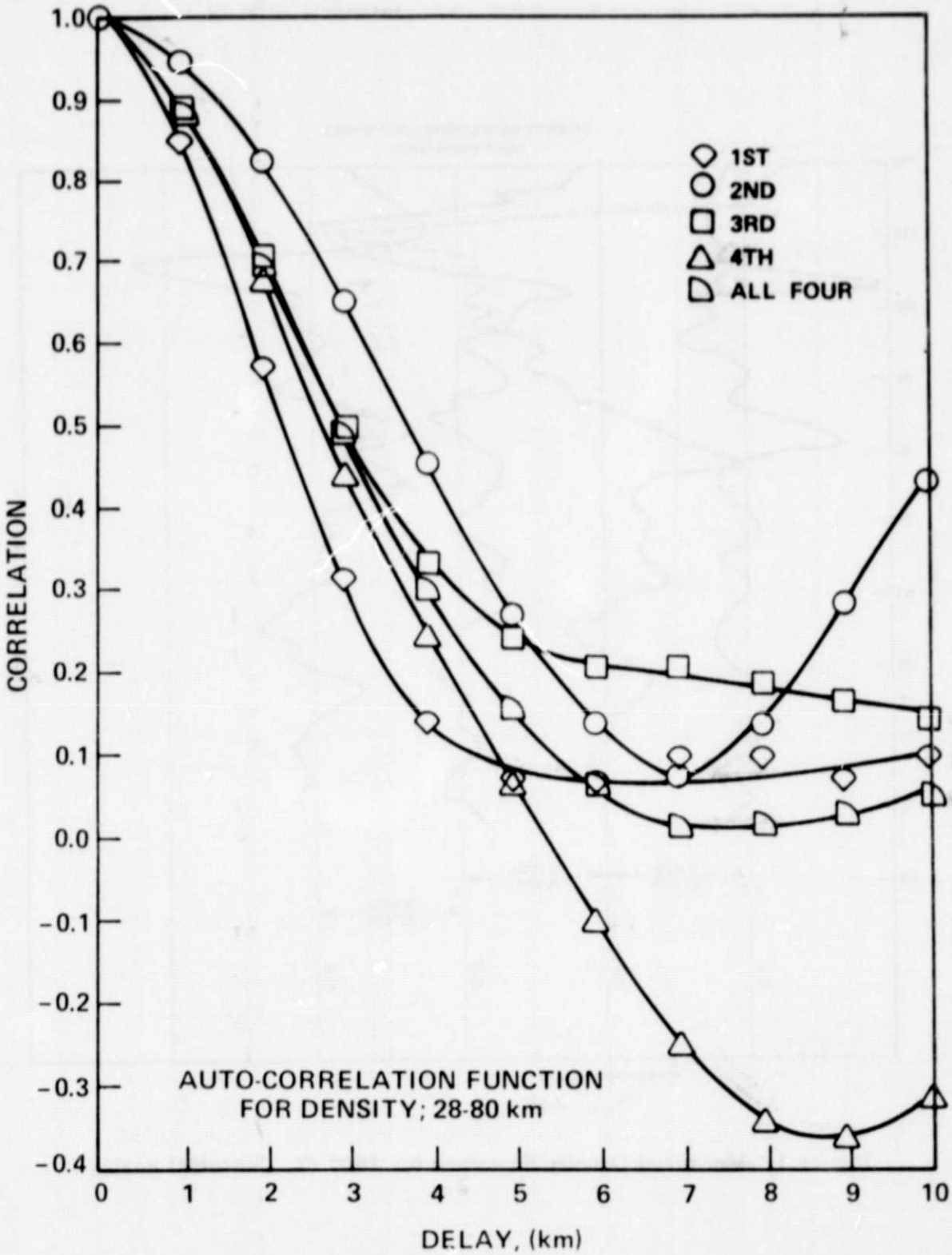

Figure 5. Spatial Auto-Correlation Functions for Density, 1967 Series

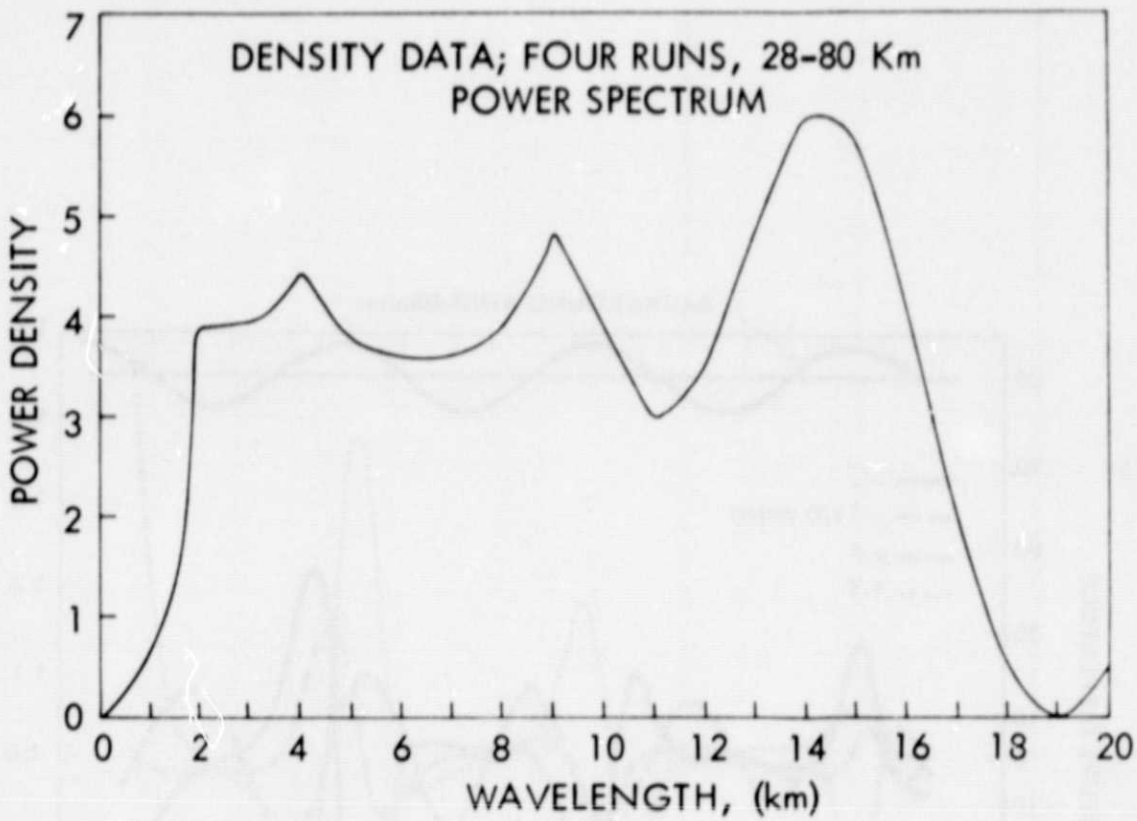

Figure 6. Power Spectral Density Versus Wavelength for Experimental Deviations, 1967 Series

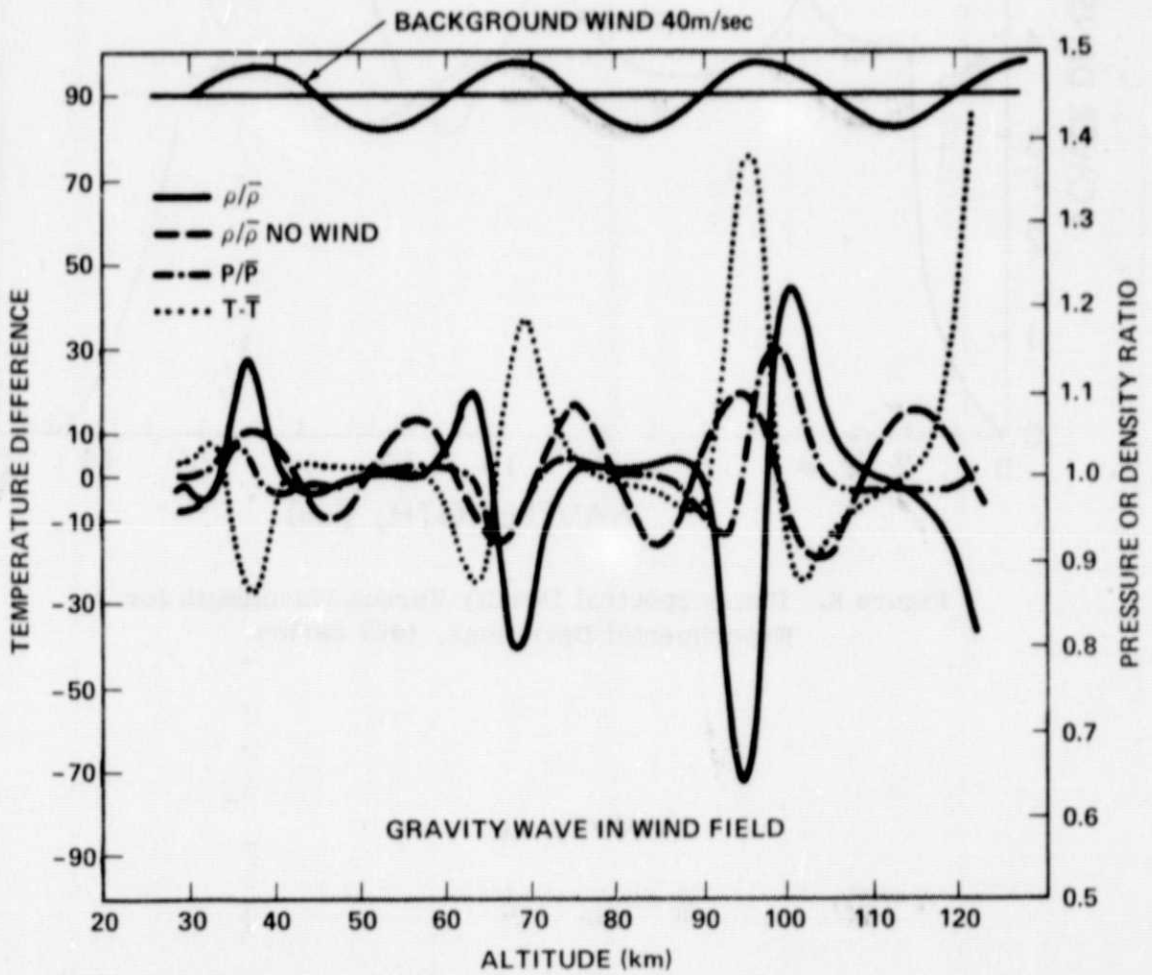

Figure 7. Gravity Wave Comparable to Measured Vertical Density Deviation for 1967 Series

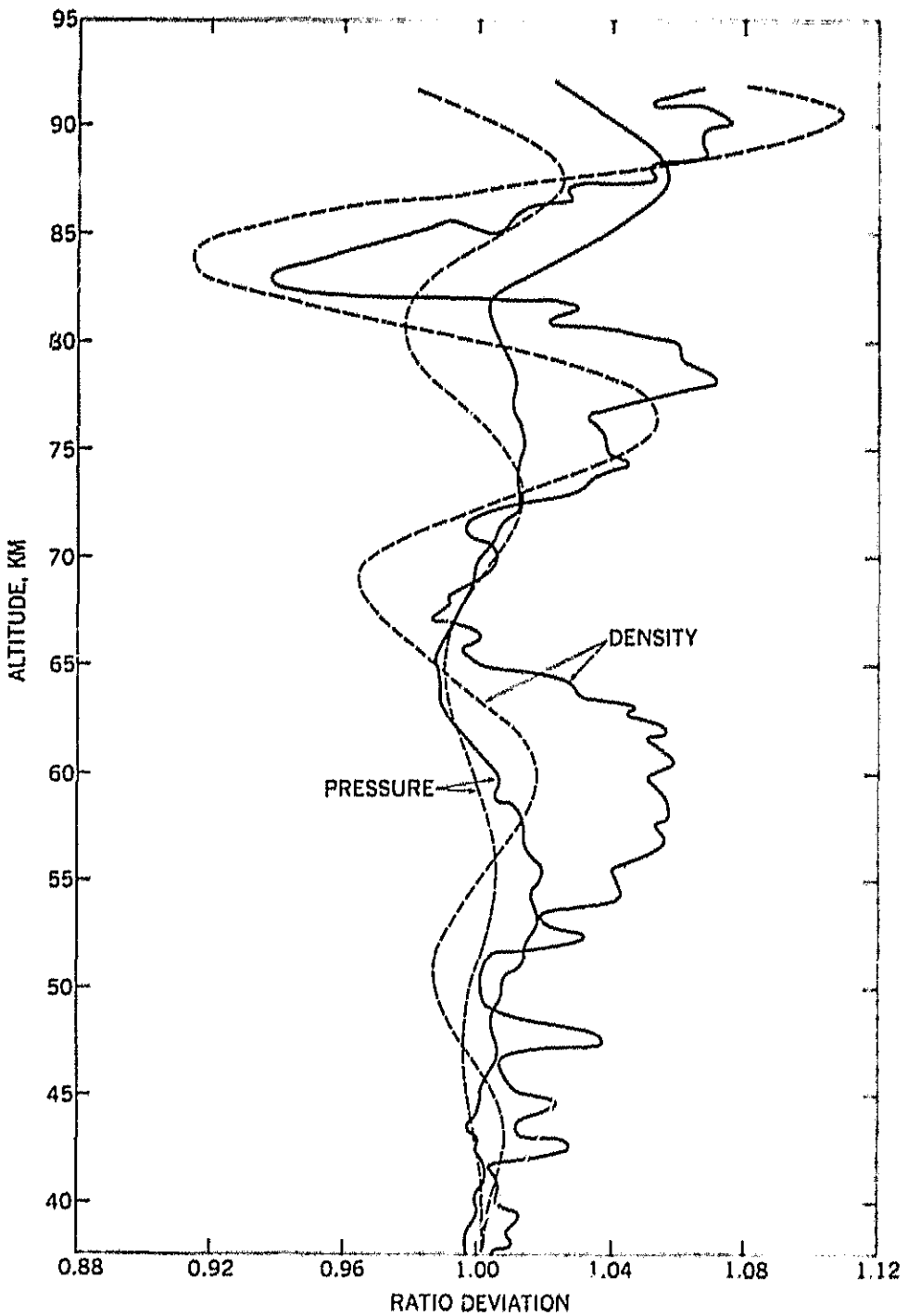

Figure 8. The Observed Pressure and Density Perturbations (Solid Curves) Over Churchill on January 13-14, 1970 Compared With the Perturbations Calculated From Theory (Broken Curves) as a Function of Altitude

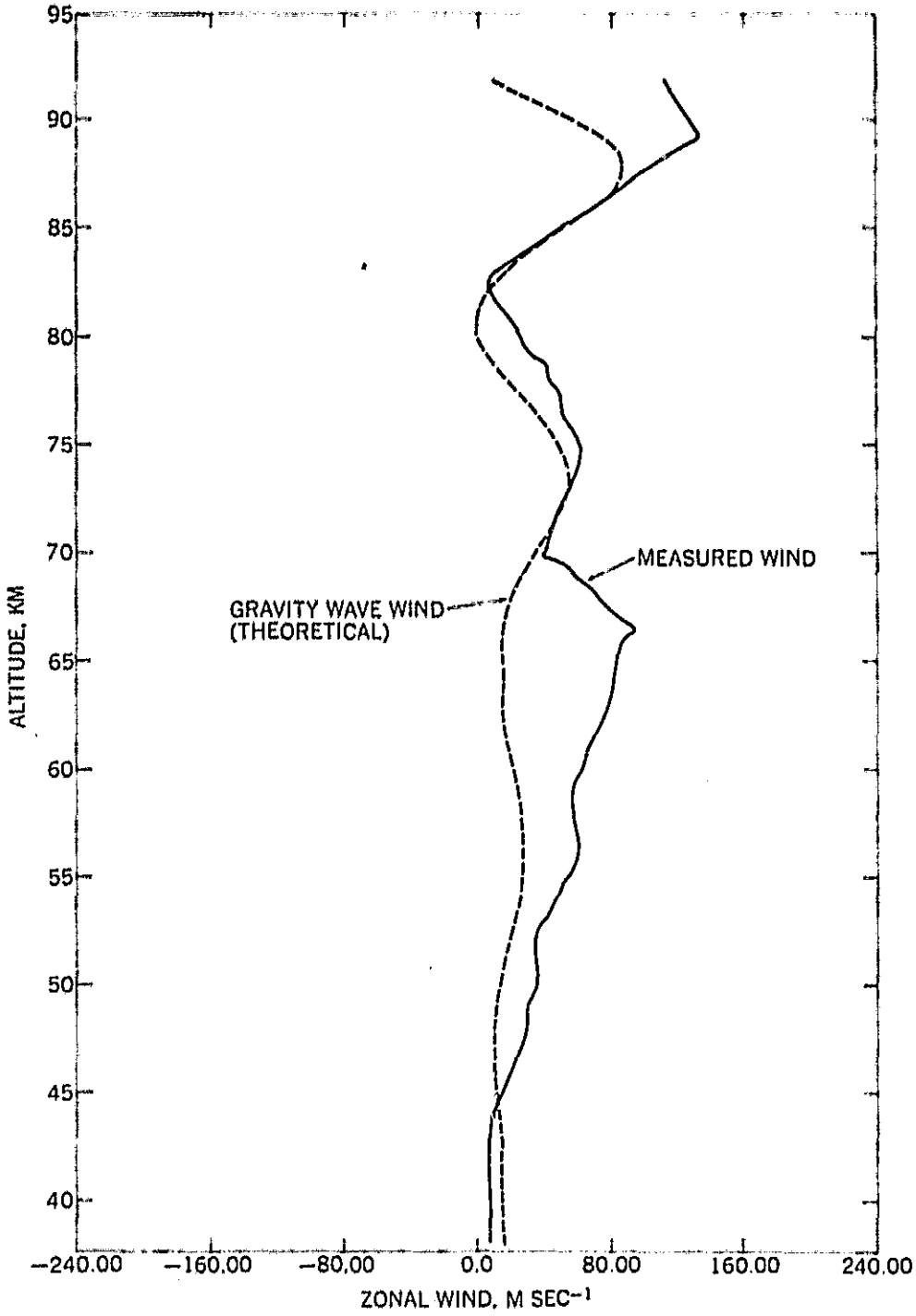

Figure 9. The Observed Zonal Wind Component Compared With the Zonal Wind Profile Calculated From the Theory for the Described Experiment

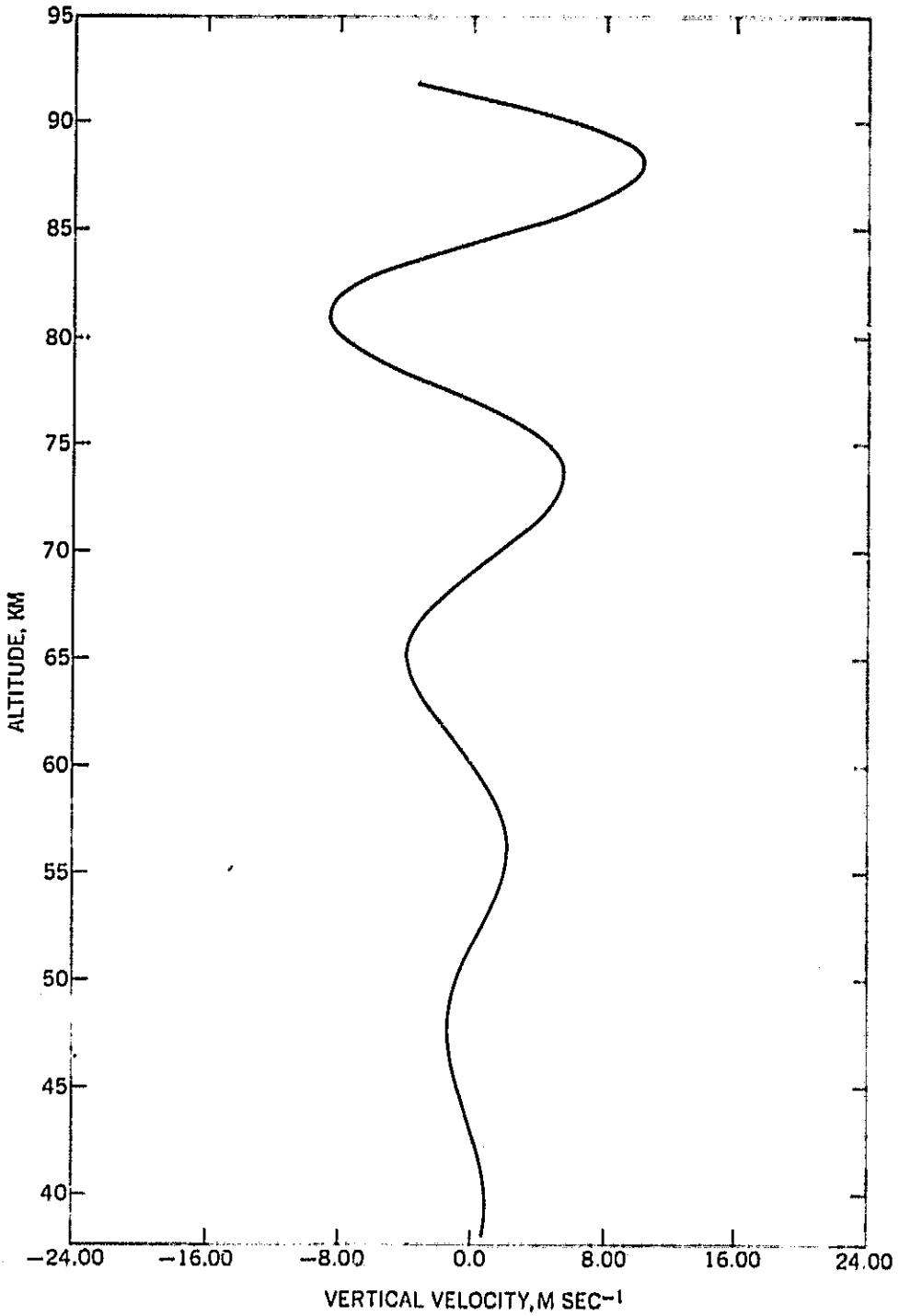

Figure 10. The Theoretical Vertical Velocity Profile Which is Consistent with the Gravity Wave Given by Figures 8-9

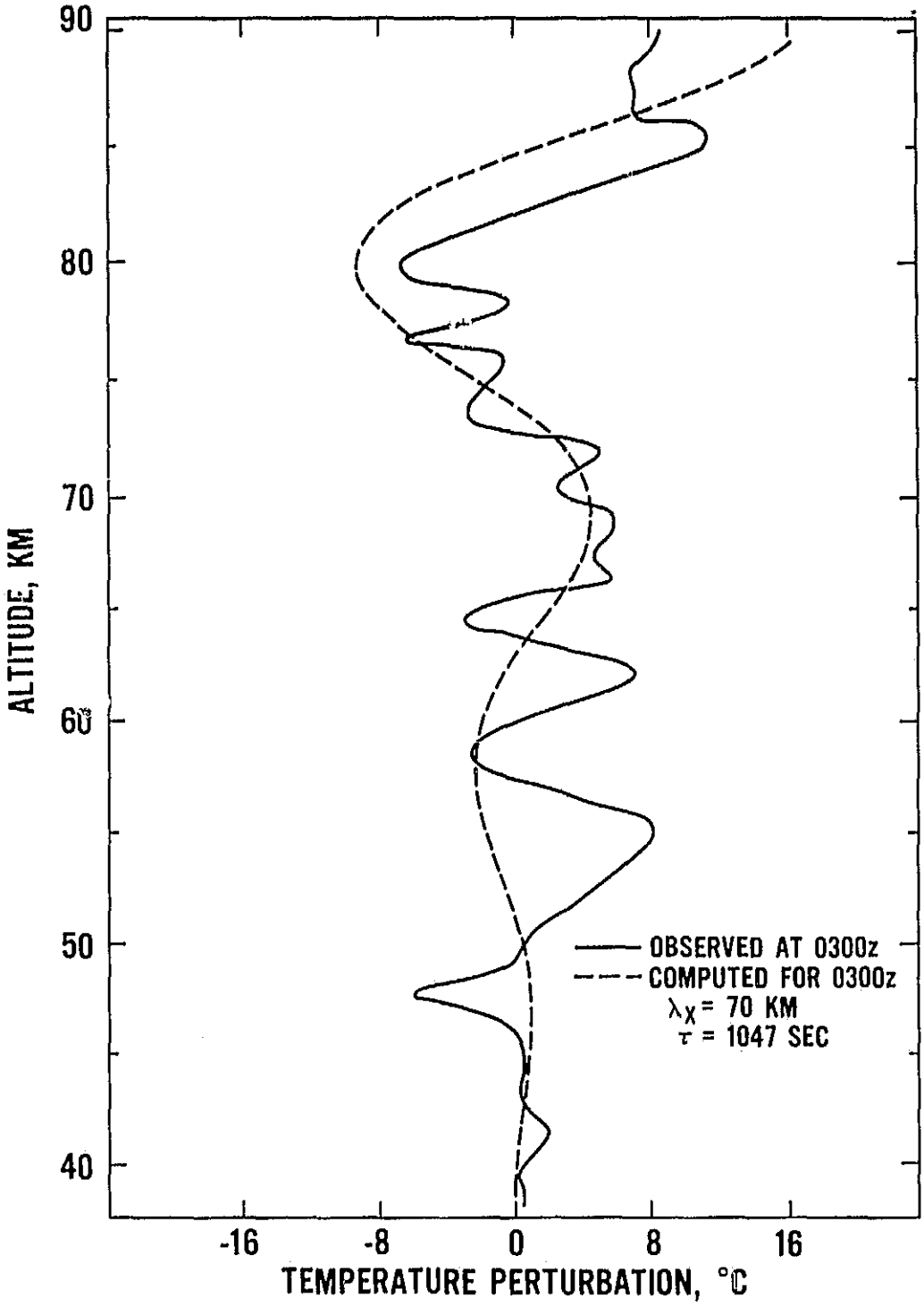

Figure 11. 1971 Series Gravity Wave Matched to First Pitot Temperature Deviation

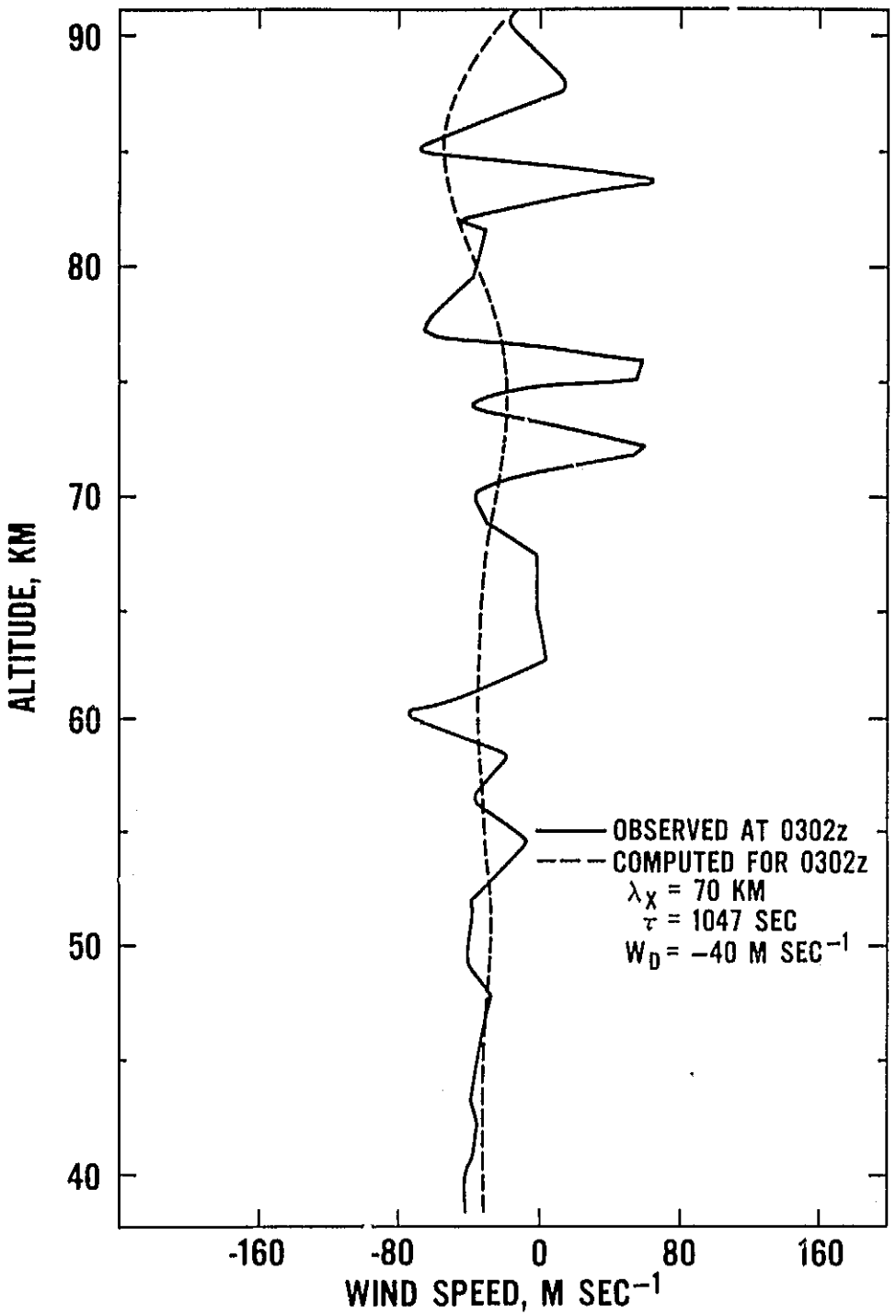

Figure 12. Comparison Between Theoretical and Observed Wind Patterns for 1971 Series

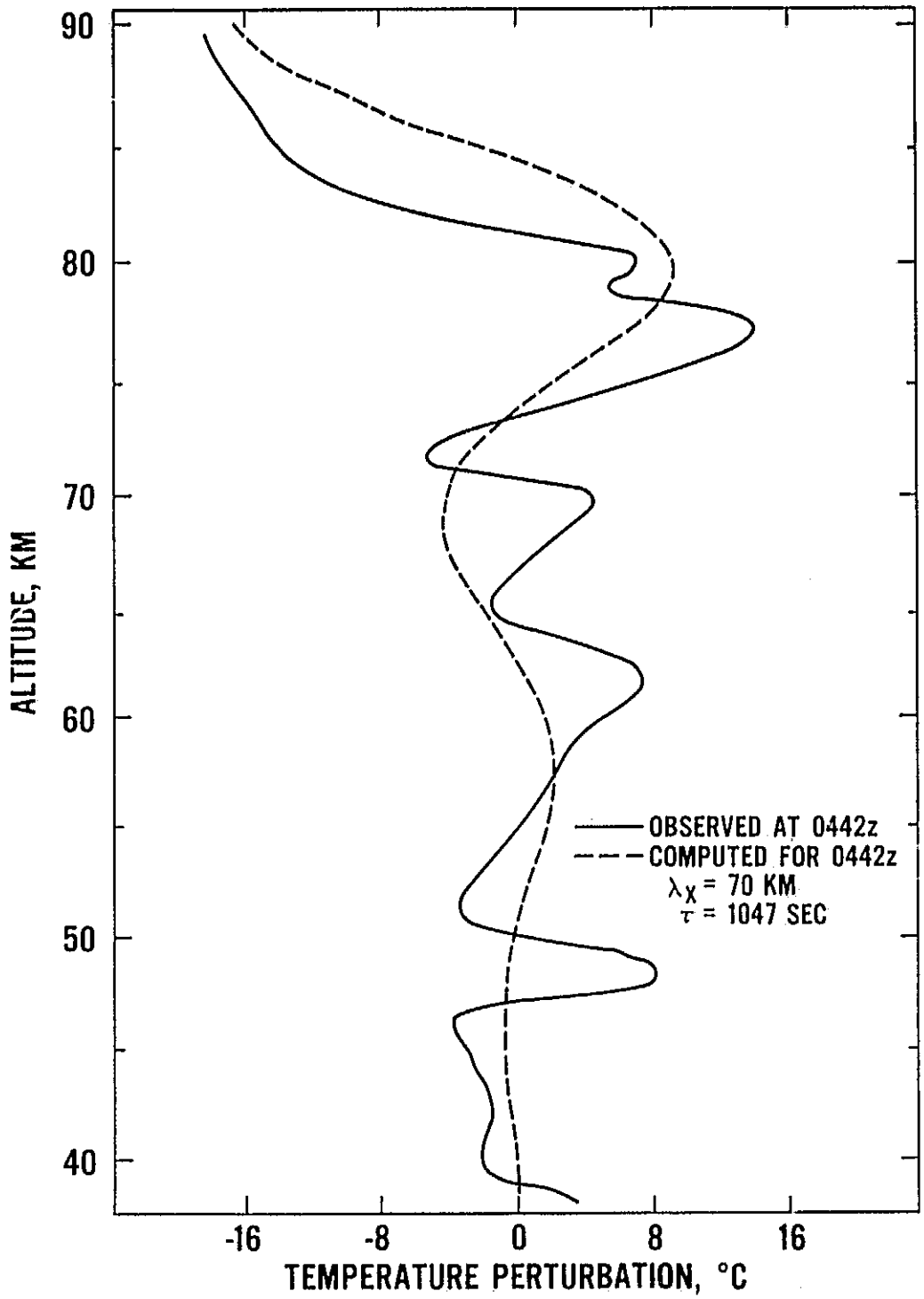

Figure 13. Comparison of Second Pitot Temperature Deviation with Gravity Wave Prediction for 1971 Series

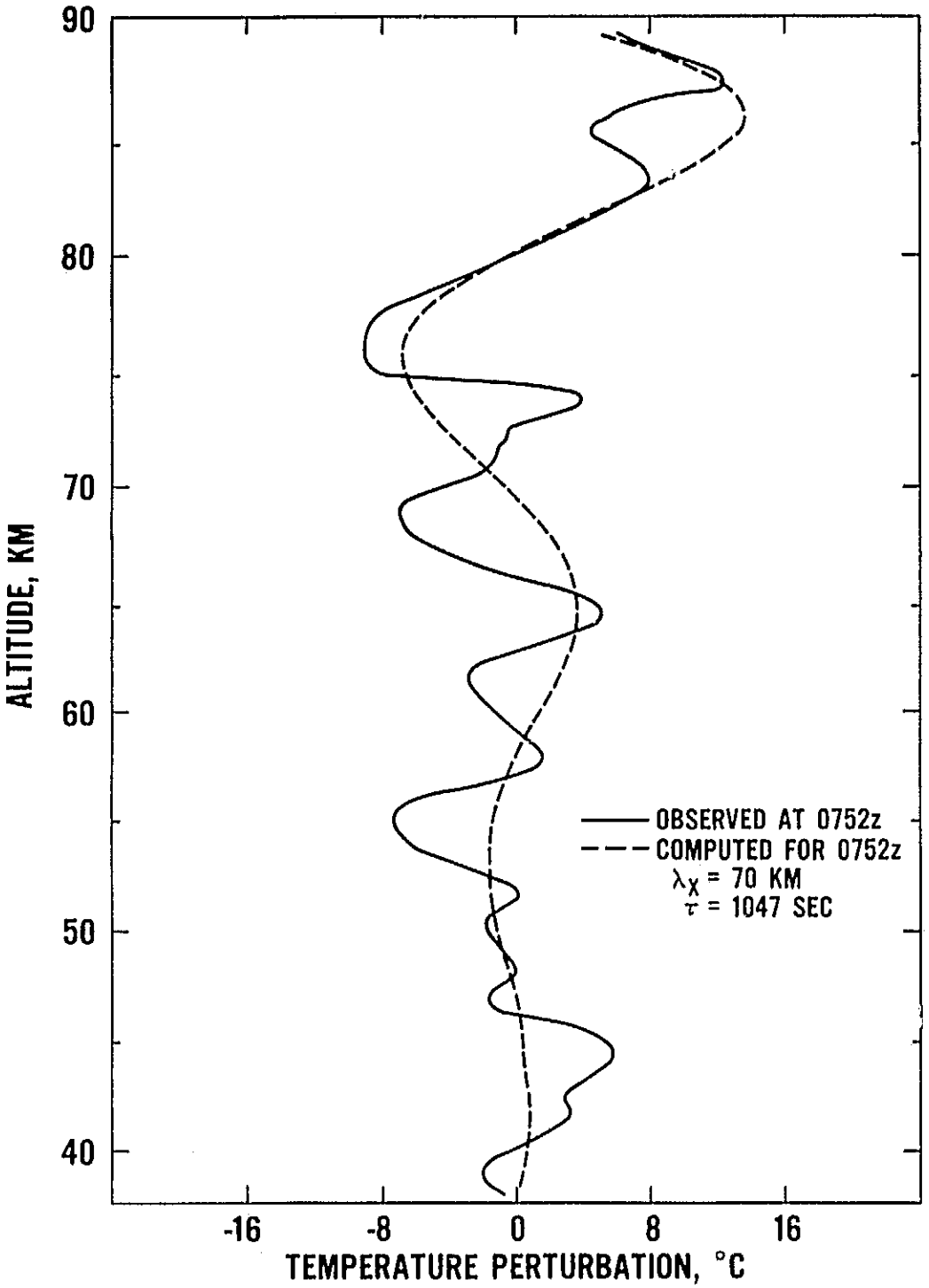

Figure 14. Comparison of Third Pitot Temperature Deviation with Gravity Wave Prediction for 1967 Series

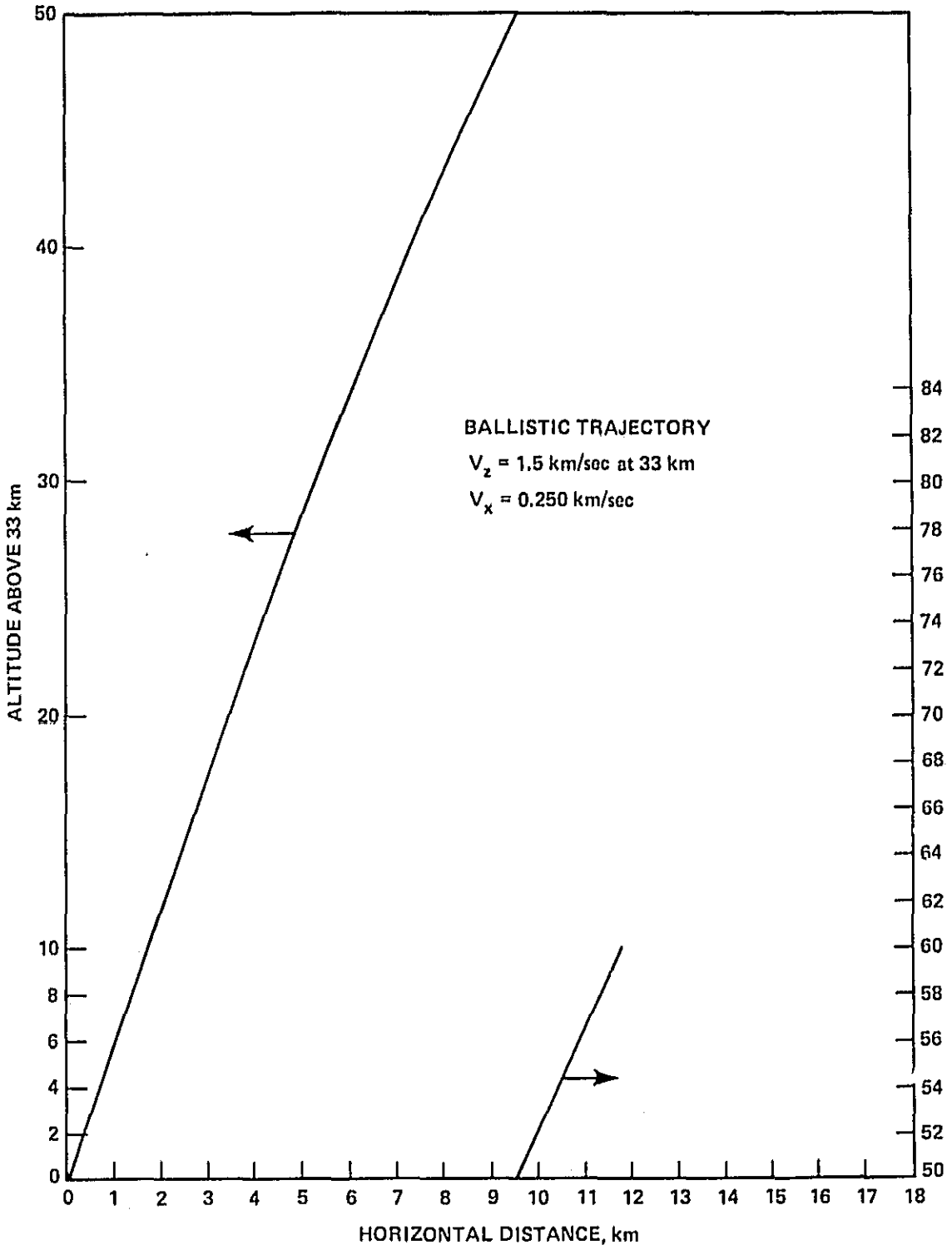

Figure 15. Typical Pitot Probe Trajectory

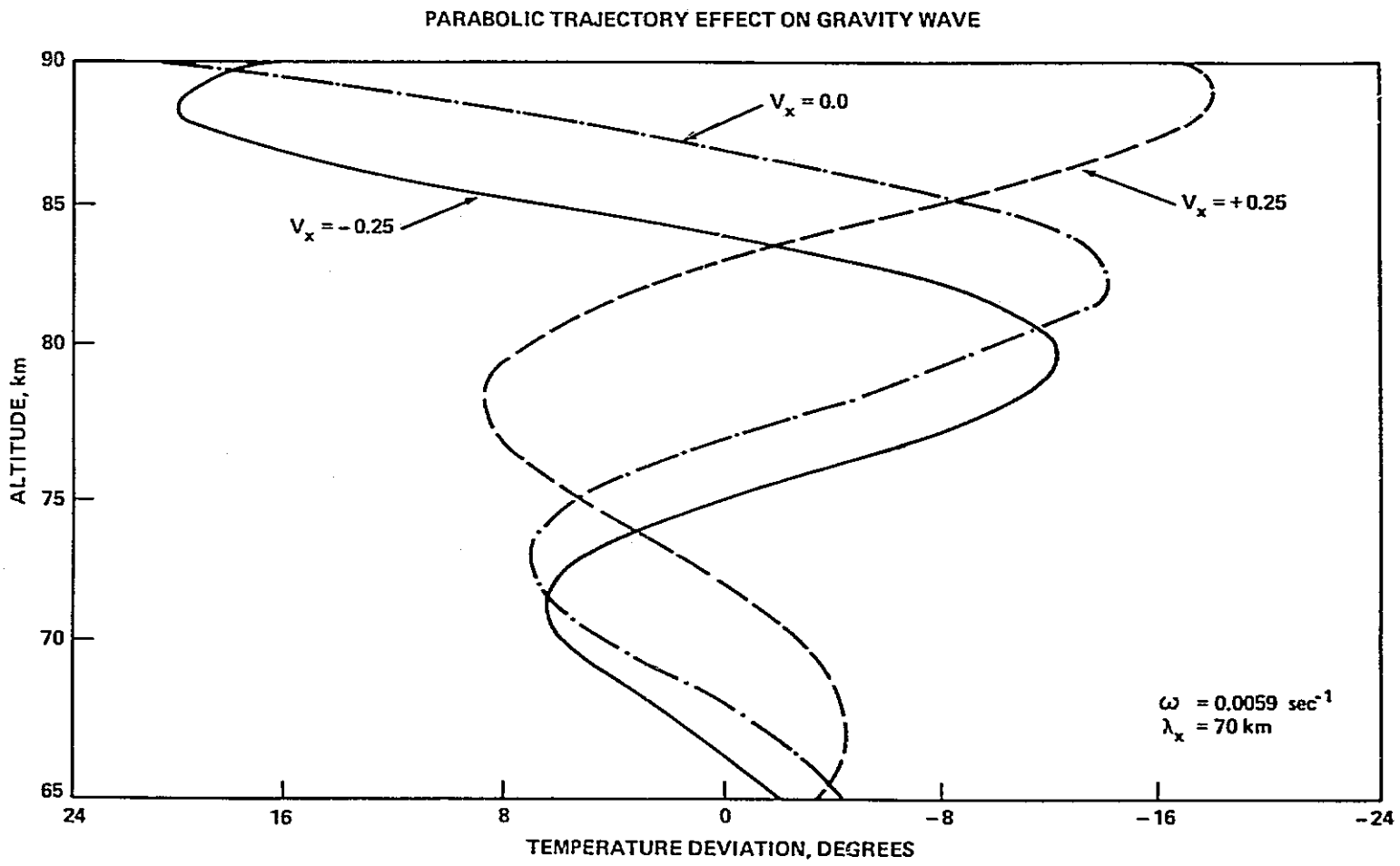

Figure 16. Gravity Wave Doppler Effect